This article was downloaded by: [Xian Jiaotong University]
On: 11 December 2014, At: 13:23
Publisher: Taylor & Francis
Informa Ltd Registered in England and Wales Registered Number: 1072954 Registered office: Mortimer House, 37-41 Mortimer Street, London W1T 3JH, UK

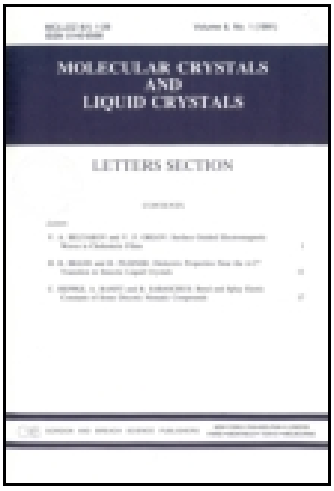

Molecular Crystals and Liquid Crystals
Publication details, including instructions for authors and subscription information:
http://www.tandfonline.com/loi/gmcl20

Theoretical Design Study on the Electronic Structures and Phosphorescent Properties of Four Iridium(III) Complexes

Deming Han[a], Xiaohong Shang[b], Gang Zhang[c] & Lihui Zhao[a]

[a] School of Life Science and Technology, International Joint Research Center for Nanophotonics and Biophotonics, Changchun University of Science and Technology, Changchun, 130022, P.R. China

[b] College of Chemistry and Life Science, Changchun University of Technology, Changchun, 130024, P.R. China

[c] State Key Laboratory of Theoretical and Computational Chemistry, Institute of Theoretical Chemistry, Jilin University, Changchun, , 130023, P.R. China

Published online: 28 Apr 2014.

To cite this article: Deming Han, Xiaohong Shang, Gang Zhang & Lihui Zhao (2014) Theoretical Design Study on the Electronic Structures and Phosphorescent Properties of Four Iridium(III) Complexes, Molecular Crystals and Liquid Crystals, 592:1, 237-248, DOI: 10.1080/15421406.2013.858025

To link to this article: http://dx.doi.org/10.1080/15421406.2013.858025

PLEASE SCROLL DOWN FOR ARTICLE

Taylor & Francis makes every effort to ensure the accuracy of all the information (the "Content") contained in the publications on our platform. However, Taylor & Francis, our agents, and our licensors make no representations or warranties whatsoever as to the accuracy, completeness, or suitability for any purpose of the Content. Any opinions and views expressed in this publication are the opinions and views of the authors, and are not the views of or endorsed by Taylor & Francis. The accuracy of the Content should not be relied upon and should be independently verified with primary sources of information. Taylor and Francis shall not be liable for any losses, actions, claims, proceedings, demands, costs, expenses, damages, and other liabilities whatsoever or howsoever caused arising directly or indirectly in connection with, in relation to or arising out of the use of the Content.

This article may be used for research, teaching, and private study purposes. Any substantial or systematic reproduction, redistribution, reselling, loan, sub-licensing, systematic supply, or distribution in any form to anyone is expressly forbidden. Terms &

Conditions of access and use can be found at http://www.tandfonline.com/page/terms-and-conditions

Downloaded by [Xian Jiaotong University] at 13:23 11 December 2014

Mol. Cryst. Liq. Cryst., Vol. 592: pp. 237–248, 2014
Copyright © Taylor & Francis Group, LLC
ISSN: 1542-1406 print/1563-5287 online
DOI: 10.1080/15421406.2013.858025

Downloaded by [Xian Jiaotong University] at 13:23 11 December 2014

Theoretical Design Study on the Electronic Structures and Phosphorescent Properties of Four Iridium(III) Complexes

DEMING HAN,[1] XIAOHONG SHANG,[2] GANG ZHANG,[3] AND LIHUI ZHAO[1,*]

[1]School of Life Science and Technology, International Joint Research Center for Nanophotonics and Biophotonics, Changchun University of Science and Technology, Changchun 130022, P.R. China
[2]College of Chemistry and Life Science, Changchun University of Technology, Changchun 130024, P.R. China
[3]State Key Laboratory of Theoretical and Computational Chemistry, Institute of Theoretical Chemistry, Jilin University, Changchun 130023, P.R. China

The geometry structures, electronic structures, absorption, and phosphorescent properties of four Ir(III) complexes have been investigated using the density functional method. Calculations of ionization potential (IP) and electron affinity (EA) were used to evaluate the injection abilities of holes and electrons into these complexes. The result also indicates that the –CF_3 substituent group on the ligand not only change the character of transition but affect the rate and balance of charge transfer. The lowest energy absorption wavelengths are located at 428 nm for ***1a****, 446 nm for* ***1b****, 385 nm for* ***2a****, and 399 nm for* ***2b****, respectively, in good agreement with the energy gap ($\Delta E_{L\text{-}H}$) trend because the HOMO–LUMO transition configurations are predominantly responsible for the $S_0 \rightarrow S_1$ transition.* ***2b*** *has the 433 nm blue emission, which might be a potential candidate for blue emitters in phosphorescent dopant emitters in organic light emitting diodes (OLEDs). The study could provide constructive information for designing novel OLEDs materials in the future.*

[Supplemental materials are available for this article. Go to the publisher's online edition of Molecular Crystals and Liquid Crystals to view the free supplemental file.]

Keywords DFT; iridium; phosphorescence; TDDFT

1. Introduction

It is well-known that phosphorescent transition-metal complexes have attracted much attention in the fabrication of organic light emitting diodes (OLEDs), which exhibits the high phosphorescence emission quantum yields at room temperature, short excited

*Address correspondence to Lihui Zhao, School of Life Science and Technology, International Joint Research Center for Nanophotonics and Biophotonics, Changchun University of Science and Technology, Changchun 130022, Jilin, P.R. China+86-431-85583023; +86-431-85583099. E-mail: zhaolihui@yahoo.com

triplet state lifetime, and photochemical stability [1–5]. It is important to design efficient phosphorescent dopants to emit the three primary colors (i.e., red, green, and blue). To do so, the most common approach is to graft various electron-withdrawing or electron-donating substituents at different positions of the coordinated ligands [8–11].

Indeed, cyclometalated iridium(III) complexes are the promising candidates as OLEDs phosphors due to the phosphorescent emission spanning the whole visible spectrum. With respect to red and green phosphorescent iridium(III) complexes, blue-emitting ones with high efficiency and good stability are still in great shortage owing to the intrinsic characteristic of the wide energy gap required between the excited triplet state and the ground state [12–14]. The addition of electron-withdrawing groups such as fluorine and trifluoromethyl to the phenyl ring has been used as one way to modulate the emission energy of iridium(III) complexes [15–19]. It is known that oxadiazole derivatives are good candidates for electron transporting and hole blocking materials in OLEDs due to the high electron affinities (EAs) [20–22]. It is also necessary to investigate further metal complexes with oxadiazole substituents to search for phosphorescent materials with good OLEDs performances.

In this study, four Ir(III) complexes **1a**, **1b**, **2a**, and **2b** with the same ancillary ligand acetylacetonate (acac) and different main ligand have been investigated using the density functional theory (DFT) and time-dependent density functional theory (TDDFT). Comparison of electronic structures and spectral properties for the four complexes was carried out. This study could provide useful information for both fundamental research and practical applications in OLEDs in the future.

2. Computational Details

The ground state geometry for each molecule was optimized by the density functional theory (DFT) [23] method with Becke's three parameter hybrid method combined with the Lee–Yang–Parr correlation functional (denoted as B3LYP) [24, 25]. The geometry optimizations of the lowest triplet states (T_1) were performed by unrestricted B3LYP approach. On the basis of the ground- and excited-state equilibrium geometries, the time-dependent DFT (TDDFT) approach associated with the polarized continuum model (PCM) in dichloromethane (CH_2Cl_2) media was applied to investigate the absorption and emission spectral properties. The "double-ξ" quality basis set LANL2DZ [26, 27] associated with the pseudopotential was employed on atom Ir. The 6-31+G(d) basis set was used for nonmetal atoms in the gradient optimizations. Furthermore, the stable configurations of these complexes can be confirmed by frequency analysis, in which no imaginary frequency was found for all configurations at the energy minima. In addition, the positive and negative ions with regard to the "electron–hole" creation are relevant to their use as OLEDs materials. Thus, ionization potentials (IP), electron affinities (EA), and reorganization energy (λ) were obtained by comparing the energy levels of neutral molecule with positive ions and negative ions, respectively. The calculated electronic density plots for frontier molecular orbitals were prepared by using the GaussView 5.0.8 software. The simulated absorption spectra are obtained by using the GaussSum 2.5 software [28]. Recent calculations with the above-mentioned methods and basis sets for transition metal complexes have supported their reliability and gave good agreement with experimental results [29, 30]. All calculations were performed with the Gaussian 09 software package [31].

Downloaded by [Xian Jiaotong University] at 13:23 11 December 2014

Downloaded by [Xian Jiaotong University] at 13:23 11 December 2014

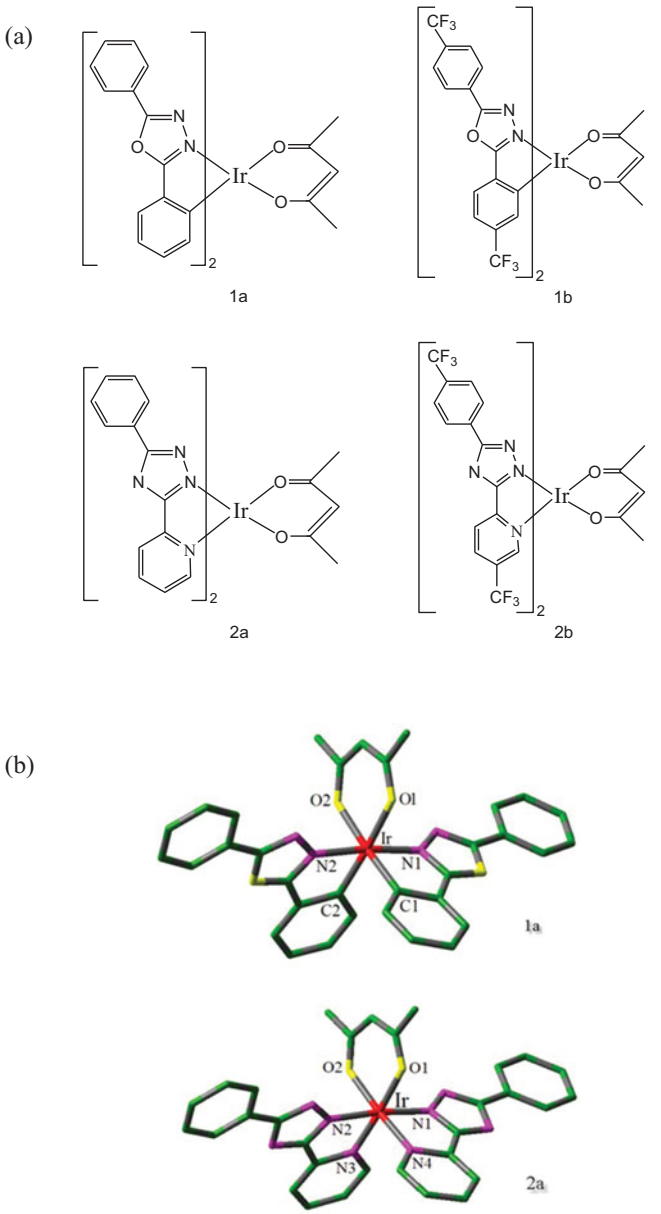

Figure 1. (a) Sketch map of the structures of iridium(III) complexes **1a**, **1b**, **2a**, and **2b**. (b) Representative optimized structure of **1a** and **2a** (H atoms omitted).

3. Results and Discussion

3.1. Geometries in the Ground State S_0 and Triplet Excited State T_1

The sketch map of the four complexes **1a**, **1b**, **2a**, and **2b** are presented in Fig. 1(a), and the optimized ground state geometric structure for **1a** and **2a** are shown in Fig. 1(b) along

with the numbering of some key atoms. The main geometric parameters in the ground and lowest triplet states are summarized in Table 1. Iridium(III) with d^6 configuration adopts a pseudo-octahedral coordination geometry surrounded by the two main ligands and one ancillary ligand. Table 1 also shows that the introduction of $-CF_3$ substituent for complexes **1b** (**2b**) makes the Ir–N1 and Ir–N2 bond distances short with respect to that of **1a** (**2a**). From **1a** (**2a**) to **1b** (**2b**), the bond angles of O1–Ir–O2 are slightly larger. For example, the bond angles of O1–Ir–O2 for **1b** (88.25 deg) is relative to the 87.92 deg for **1a**.

From the S_0 to T_1 states, the bond distances of Ir–N1 in the four complexes are shortened significantly (by 0.0569, 0.0528, 0.0298, 0.0285 Å, respectively), which will strengthen the interaction between the iridium atom and the corresponding ligand.

In addition, for **1a** and **1b**, the bond distances of Ir–N2 are extended, exhibiting the opposite trend with respect to that of **2a** and **2b**. Meanwhile, the bond angle of O1–Ir–O2, O2–Ir–C1(N4), O1–Ir–C2(N3), and N1–Ir–N2 in T_1 states are slightly smaller compared with the S_0 ones. In addition, the dihedral angles of N1–Ir–O1–O2 in T_1 states are also slightly smaller than that of the S_0 ones.

3.2. Molecular Orbital Properties

It is well-known that the properties of the excited states and electronic transitions of organic light-emitting materials are closely related to the characters of the frontier molecular orbitals (FMOs), especially highest occupied molecular orbital (HOMO) and lowest unoccupied molecular orbital (LUMO). The HOMO and LUMO distribution, energy levels, and energy gaps between of LUMO and HOMO ($\Delta E_{L\rightarrow H}$) of the four complexes **1a**, **1b**, **2a**, and **2b** are plotted in Fig. 2. The calculated FMO compositions for **1a**, **1b**, **2a**, and **2b** were listed in Tables S1–S4 (Supplemental material).

It is known that the electron-withdrawing groups can make the energies of HOMOs and LUMOs decrease, which can be seen from Fig. 2. For example, due to the $-CF_3$ substituent incorporated at the 4-positions of the phenyl rings, **1b** has the smaller values of HOMO(−5.66 eV) and LUMO(−2.41 eV) with respect to those of **1a**. In addition, **1b** and **2a** have the smallest and largest $\Delta E_{L\text{-}H}$ value among the four complexes, respectively. From Table 2, it can be seen that **1a** and **1b** have the similar LUMO distributions and different HOMO distributions, that is, the electron densities of HOMO for **1b** localized on the Ir atom (20%) and ancillary ligand (75%) with respect to the distribution on Ir atom (46%) and two main ligands (48%) for **1a**. However, **2a** and **2b** have the similar HOMO and LUMO distributions predominantly localized on two main ligands, indicating the $-CF_3$ substituent has slightly effect on the electronic structure of **2b**.

3.3. Ionization Potential (IP) and Electronic Affinity (EA)

It is known that IP, electron affinity (EA), and migration of charge are the three key factors for designing optoelectronic materials. A larger EA (smaller IP) indicates easier injection of electrons (holes) into the emitting materials from the electron (hole) transporting layer. The reorganization energy (λ) can evaluate the charge transfer rate and balance. For photoluminescent materials, a smaller IP value means easier hole injection ability and a larger EA value will facilitate electron injection. We also calculated the hole extraction potential (HEP), which is the energy difference between M (neutral molecule) and M^+ (cationic), using M^+ geometry, and electron extraction potential (EEP), which is the energy difference between M and M^- (anionic), using M^- geometry. The calculated vertical IP (IP_v), adiabatic IP (IP_a), vertical EA (EA_v), adiabatic EA (EA_a), HEP, and EEP are listed

Downloaded by [Xian Jiaotong University] at 13:23 11 December 2014

Downloaded by [Xian Jiaotong University] at 13:23 11 December 2014

Table 1. Main optimized geometry parameters for complexes **1a**, **1b**, **2a**, and **2b**

	1a		1b		2a		2b	
	S_0	T_1	S_0	T_1	S_0	T_1	S_0	T_1
Bond length (Å)								
Ir–C1(N4)	2.0297	2.0112	2.0291	2.0079	2.0799	2.0572	2.0835	2.0637
Ir–C2(N3)	2.0297	2.0348	2.0291	2.0354	2.0799	2.0572	2.0835	2.0636
Ir–N1	2.0508	1.9939	2.0490	1.9962	2.0510	2.0212	2.0482	2.0197
Ir–N2	2.0508	2.0770	2.0490	2.0756	2.0510	2.0212	2.0482	2.0198
Ir–O1	2.1672	2.1583	2.1585	2.1468	2.0521	2.0645	2.0472	2.0542
Ir–O2	2.1672	2.1740	2.1585	2.1655	2.0521	2.0645	2.0472	2.0542
Bond angle (deg)								
O1–Ir–O2	87.92	87.55	88.25	87.58	93.40	92.26	93.58	92.59
C1(N4)–Ir–N1	79.50	81.25	79.46	81.20	78.69	79.41	78.67	79.40
C2(N3)–Ir–N2	79.50	79.43	79.46	79.44	78.69	79.41	78.67	79.40
O1–Ir–C2(N3)	175.60	174.82	175.45	174.63	175.56	174.10	175.33	174.10
O2–Ir–C1(N4)	175.60	175.26	175.46	174.81	175.56	174.10	175.33	174.10
N1–Ir–N2	173.96	173.94	173.89	173.68	171.58	170.22	172.30	170.07
Dihedral angle (deg)								
N1–Ir–O1–O2	96.73	95.09	96.59	94.80	96.88	95.39	96.67	95.24
C1–C2–O1–O2	172.64	171.48	172.30	170.91	—	—	—	—
N4–N3–O1–O2	—	—	—	—	171.33	169.52	170.95	169.14

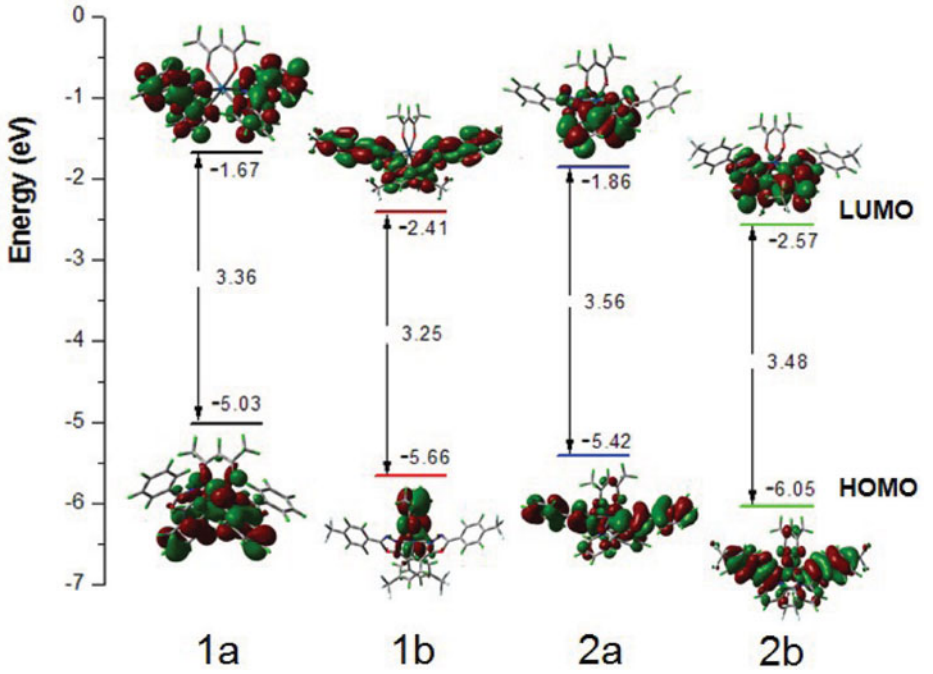

Figure 2. Molecular orbital diagrams and HOMO and LUMO energies for complexes **1a, 1b, 2a, and 2b**.

in Table 2. The IP_v is defined as the energy difference between the cation and its neutral molecule at the equilibrium geometry of the neutral molecule. The IP_a is defined as the energy difference between the cation and its neutral molecule at their own equilibrium geometries. The EA_v is defined as the energy difference between the neutral molecule and its anion both at the equilibrium geometry of the anion. The EA_a is defined as the energy difference between the neutral molecule and its anion at their own equilibrium geometries.

The complex **1b** with the $-CF_3$ substituent incorporated at the 4-positions of the phenyl rings revealed obviously larger IP and EA values with respect to **1a**, attributed to the strong electron-withdrawing ability of $-CF_3$. This is also found to compare **2b** to **2a**. In addition, the complex **1a** and **2b** have the smallest IP value and largest EA value among the four

Table 2. The calculated vertical IP (IP_v), adiabatic IP (IP_a), HEP, vertical EA (EA_v), and adiabatic EA (EA_a), EEP, and reorganization energies for electron ($\lambda_{electron}$) and hole (λ_{hole}) for each complex (Unit: eV)

	IP_v	IP_a	HEP	EA_v	EA_a	EEP	$\lambda_{electron}$	λ_{hole}
1a	6.407	6.291	6.174	0.597	0.681	0.765	0.167	0.233
1b	6.806	6.655	6.523	1.374	1.484	1.595	0.220	0.283
2a	6.510	6.416	6.319	0.640	0.742	0.849	0.209	0.191
2b	7.103	6.992	6.880	1.399	1.548	1.676	0.276	0.223

Downloaded by [Xian Jiaotong University] at 13:23 11 December 2014

Downloaded by [Xian Jiaotong University] at 13:23 11 December 2014

Table 3. Phosphorescent emissions of **1a**, **1b**, **2a**, and **2b** in CH_2Cl_2 at the TDDFT calculations, together with experimental wavelength available

	B3LYP λ(nm)/*E*(eV)	Configuration	M062X λ(nm)/*E*(eV)	Configuration	Nature	Exptl.[a]
1a	642/1.92	L→H(71%)	534/2.31	L→H(74%)	^{3}LMCT/^{3}LLCT π^*(B)→d(Ir)+π(A+B)	529 (nm)
		L→H-2(18%)		L→H-2(14%)	^{3}LMCT/^{3}LLCT π^*(B)→d(Ir)+π(A+B)	
1b	660/1.87	L→H(71%)	540/2.29	L→H(57%)	^{3}LMCT/^{3}LLCT π^*(B)→d(Ir)+π(A+B)	
		L→H-2(21%)		L→H-2(18%)	^{3}LMCT/^{3}LLCT π^*(B)→d(Ir)+π(A+B)	
2a	502/2.46	L→H(67%) L+1→H-1(23%)	419/2.95	L→H(45%) L+1→H-1(29%)	^{3}LMCT/^{3}LLCT/^{3}ILCT π^*(B)→d(Ir)+π(A+B)^{3}ILCT π^*(B)→π(B)	
2b	523/2.36	L→H(70%)	433/2.86	L→H(47%)	^{3}LMCT/^{3}LLCT/^{3}ILCT π^*(B)→d(Ir)+π(A+B)	
		L+1→H-1(22%)		L+1→H-1(31%)	^{3}ILCT π^*(B)→π(B)	

[a]From Ref. [22]

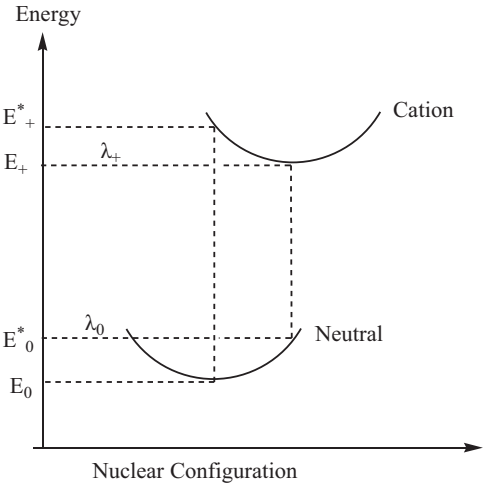

Figure 3. Schematic description of the internal reorganization energy for hole transfer.

Downloaded by [Xian Jiaotong University] at 13:23 11 December 2014

complexes, respectively, indicating that the easiest hole injection ability for **1a** and the strongest electron injection ability for **2b**.

According to the Marcus-Hush model [32–34], the charge (hole or electron) transfer rate K_{et} can be expressed by the following formula:

$$K_{et} = A\exp(-\lambda/4k_BT) \tag{1}$$

where T is the temperature, k_B is the Boltzmann constant, λ is the reorganization energy. Due to the limited intermolecular charge transfer range in the solid state, the mobility of charges has been demonstrated to be predominantly related to the internal reorganization energy λ for OLEDs materials [35–38]. Generally, λ is determined by fast changes in molecular geometry (the internal reorganization energy λ_i) and by slow variations in solvent polarization of the surrounding medium (the external reorganization energy λ_e). In OLEDs devices, the contribution from λ_e can be neglected. Therefore, the internal reorganization energy λ_i is the determinant factor. λ_i for hole transfer (λ_{hole}) can be expressed as follows [39]:

$$\lambda_{hole} = \lambda_0 + \lambda_+ = (E_0^* - E_0) + (E_+^* - E_+) = IP_v - HEP \tag{2}$$

As illustrated in Fig. 3, E_0 and E_+ represent the energies of the neutral and cationic species in their lowest energy geometries, respectively, while E_0^* and E_+^* represent the energies of the neutral and cationic species with the geometries of the cationic and neutral species, respectively, which is equal to the difference between IP_v and HEP. Similarly, the reorganization energy for electron transport ($\lambda_{electron}$) can be evaluated as: $\lambda_{electron} = EEP - EA_v$. As emitting layer materials, it needs to achieve hole and electron injection and transport balance. To the best of our knowledge, the reorganization energy (λ) can be approximately used to estimate the charge transport rate and balance between holes and electrons. The results are also listed in Table 2. The reorganization energies for hole transport (λ_{hole}) are obviously larger than electron transport ($\lambda_{electron}$), which indicates that electron transport has better performance than hole transport. In addition, one can find that complex **2a** has the best hole transfer ability with the smallest λ_{hole} value (0.191 eV) among

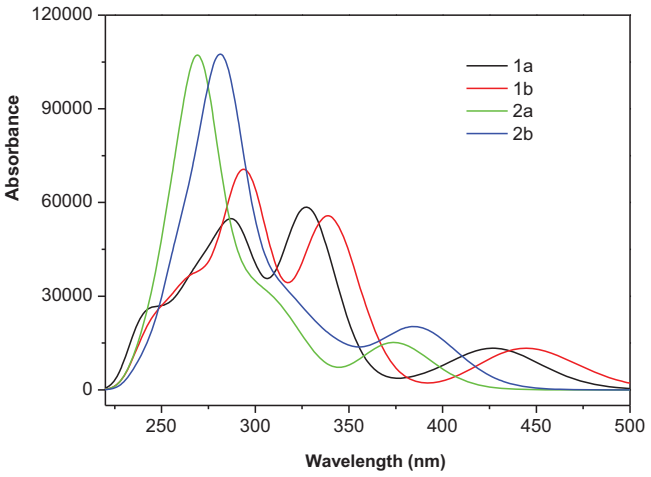

Figure 4. Simulated absorption spectra in CH_2Cl_2 for **1a**, **1b**, **2a**, and **2b**.

the four complexes. We also found that the energy differences between λ_{hole} and $\lambda_{electron}$ for **1a**, **1b**, **2a**, and **2b** are 0.066, 0.063, 0.018, and 0.053 eV, respectively. It can be seen that **2a** with the smaller λ value and the smaller differences between λ_{hole} and $\lambda_{electron}$ indicates the better transfer balance between holes and electrons. As shown in Table 2, the λ_{hole} values for **2a** and **2b** are smaller than the $\lambda_{electron}$ values, which suggests that the hole transfer rate is better than the electron transfer rate. While the difference between $\lambda_{electron}$ and λ_{hole} (0.018) for **2a** is much smaller than that of **2b** (0.053), which can greatly improve the charge transfer balance of **2a**, thus further enhancing the device performance of OLEDs. The above analysis indicates that the charge transfer rate of holes and electrons has been obviously influenced by the $-CF_3$ substituent.

3.4. Absorption Spectra

On the basis of the optimized ground state geometries, the absorption properties of **1a**, **1b**, **2a**, and **2b** were calculated using TDDFT method. The vertical electronic excitation energies, oscillator strengths (f), assignment, and configurations have been listed in Table S5 (Supplemental material). The absorption spectra of the studied complexes in CH_2Cl_2 media based on the TDDFT calculations are shown in Fig. 4.

The lowest energy absorption wavelengths are located at 428 nm ($f = 0.1728$) for **1a**, 446 nm ($f = 0.1669$) for **1b**, 385 nm ($f = 0.0259$) for **2a**, and 399 nm ($f = 0.0330$) for **2b**, respectively, in good agreement with the energy gaps ($\Delta E_{L\text{-}H}$) trend (Fig. 2) because the HOMO–LUMO transition configurations are predominantly responsible for the $S_0 \rightarrow S_1$ transition (**1a**: 94%; **1b**: 95%; **2a**: 96%; **2b**: 95%). It can be seen that the calculated 428 nm absorption for **1a** is in good agreement with the experimental value 424 nm [22]. In comparison with **1a** (**2a**), **1b** (**2b**) has the red-shifted lowest energy absorption due to the introduction of $-CF_3$ substituent, which can be rationalized by the fact that **1b** (**2b**) has the smaller $\Delta E_{L\text{-}H}$ value. As seen in Fig. 4, complexes **1a** and **1b** have similar absorption curves in the band range of 275–350 nm. Besides, **2a** and **2b** have also the similar shape at the about 275 nm, a large peak appearing.

Downloaded by [Xian Jiaotong University] at 13:23 11 December 2014

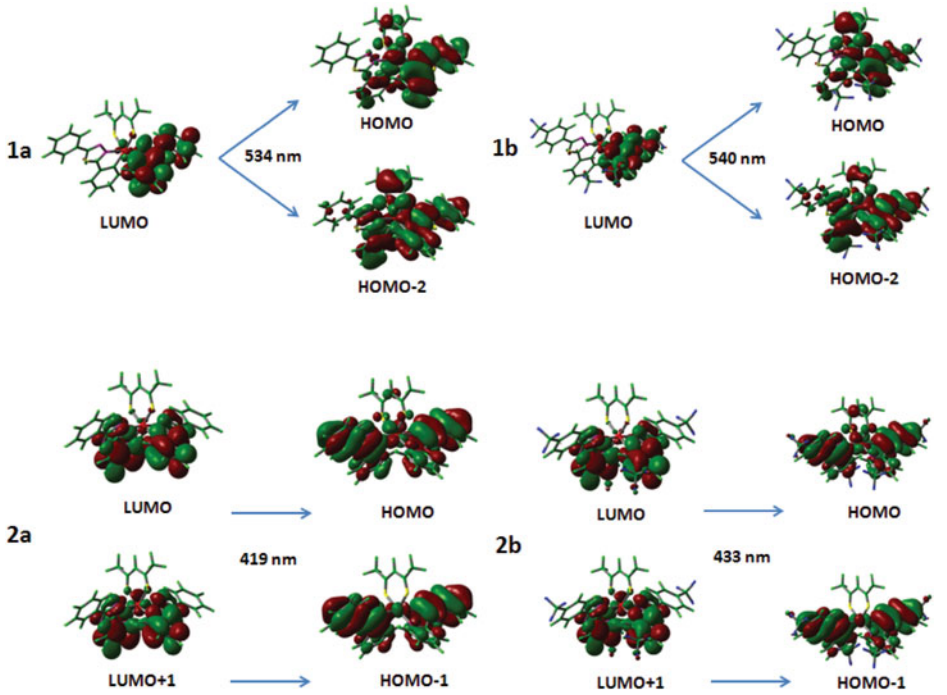

Figure 5. Transitions responsible for the emissions at 534, 540, 419, and 433/nm for complexes **1a**, **1b**, **2a**, and **2b**, respectively, simulated in CH_2Cl_2 media at the M062X level.

From the above discussion on the FMOs, the lowest energy absorptions of **1a** is assigned as metal to ligand charge transfer (MLCT)/ ligand to ligand charge transfer (LLCT)/intraligand charge transfer (ILCT) transition characters, and its maximum absorption bands is located at 428 nm described as $d(Ir)+\pi(B)\rightarrow\pi^*(B)$ transition (B denotes the two main ligands in each complex). For **1b**, the lowest absorption is ascribed to $d(Ir)+\pi(A)\rightarrow\pi^*(B)$ (A denotes the ancillary ligand in each complex) with MLCT/LLCT character. This indicates that the introduction of $-CF_3$ substituent has important effect on the transition character of the lowest energy absorptions for **1b** with respect to **1a**. In addition, the lowest energy absorptions at 385 and 399 nm for **2a** and **2b** can both be described as $d(Ir)+\pi(B)\rightarrow\pi^*(B)$ transition of MLCT/ILCT character.

3.5. Phosphorescence

On the basis of the optimized triplet excited-state (T_1) geometries, the emission properties of complexes **1a**, **1b**, **2a**, and **2b** in CH_2Cl_2 solution are shown in Table 3. To check the computational method, two different density functionals (B3LYP and M062X [40]) were used. A good agreement with experimental data were obtained for M062X, while a disagreement was found for B3LYP. The calculated lowest energy emissions for **1a**, **1b**, **2a**, and **2b** at M062X level are localized at 534, 540, 419, and 433 nm, vs. 642, 660, 502, 523 nm at B3LYP level. For **1a**, the lowest energy emission at M062X (534 nm) is in good agreement with the measured value (529 nm) vs. the significant deviation of 113 nm at B3LYP level from the experimental data [22]. The plots of the molecular orbitals related to

Downloaded by [Xian Jiaotong University] at 13:23 11 December 2014

emissions of **1a**, **1b**, **2a**, and **2b** in CH_2Cl_2 media at the M062X level are also presented in Fig. 5.

Table 3 shows that for **1a** and **1b**, at the M062X level, the phosphorescent emissions were contributed mainly by the LUMO→HOMO and LUMO→HOMO-2 transitions. Their lowest energy phosphorescent emissions have the ^{3} ligand to metal charge transfer (LMCT)/^{3} ligand to ligand charge transfer (LLCT) [π^*(B)→d(Ir)+ π(A+B)] character. For **2a** and **2b**, at the M062X level, the phosphorescent emissions were contributed mainly by the LUMO→HOMO and LUMO + 1→HOMO − 1 transitions. Their lowest energy phosphorescent emissions are mainly composed of [π^*(B)→d(Ir)+π(A+B)] [^{3}LMCT//^{3}LLCT(ligand to ligand charge transfer)/^{3}ILCT(intraligand charge transfer)] and [π^*(B)→π(B)] [^{3}ILCT]. The emissions of **2a** and **2b** are blue shifted about 110 nm compared with **1a** and **1b**, respectively, indicating that the emission properties are sensitive to the selected main ligands in these complexes. It can be seen that the emission spectra of the **2b** is in the blue region, and we expect it might be a potential candidate for blue emitters in phosphorescent dopant emitters in OLEDs. From Fig. 5, it can be seen that the LUMO of **1a** and **1b** are localized on the one main ligand different from those of **2a** and **2b**, that is, their LUMO localized on the two main ligands. Similarly, the HOMOs of **1a** and **1b** have also different distributions from those of **2a** and **2b**.

4. Conclusions

In this paper, we have applied DFT and TDDFT methods to investigate the geometries, electronic structures, injection and transporting, absorption and phosphorescence properties of four heteroleptic Ir(III) complexes. The molecular orbitals have been analyzed to study the microcosmic charge transfer transitions in absorption and emission in detail. The highest occupied orbital energies (HOMO), the lowest virtual orbital energies (LUMO), $\Delta E_{\text{L-H}}$ (the energy gaps between the LUMO and HOMO), the IP, EA, and reorganization energies (λ) were computed to evaluate the charge transfer and balance properties between hole and electron. It is noted that the $-CF_3$ substituent group on the ligand has impact on not only the character of transition but also affect the rate and balance of charge transfer. It is anticipated that the theoretical studies will be helpful in designing novel iridium(III) complexes as phosphorescent materials with good OLEDs performances.

Acknowledgments

The authors are grateful to the financial aid from the Program of Science and Technology Development Plan of Jilin Province (Grant No. 20130203032YY) and the Funds for Doctoral Scientific Research Startup of Changchun University of Science and Technology (Grant No. 40301855).

References

[1] Bolink, H. J., Coronado, E., Santamaria, S. G., Sessolo, M., Evans, N., Klein, C., Baranoff, E., Kalyanasundaram, K., Graetzel, M., & Nazeeruddin, M. K. (2007). *Chem. Commun.*, *31*, 3276.
[2] Park, G. Y., & Ha, Y. (2008). *Synthetic Met.*, *158*, 120.
[3] Lee, T. C., Hung, J. Y., Chi, Y., Cheng, Y. M., Lee, G. H., Chou, P. T., Chen, C. C., Chang, C. H., & Wu, C. C. (2009). *Adv. Funct. Mater.*, *19*, 2639.
[4] Che, C. M., Kwok, C. C., Lai, S. W., Rausch, A. F., Finkenzeller, W. J., Zhu, N. Y., & Yersin, H. (2010). *Chem. Eur. J.*, *16*, 233.

Downloaded by [Xian Jiaotong University] at 13:23 11 December 2014

[5] Tao, S. L., Lai, S. L., Wu, C. A., Ng, T. W., Chan, M. Y., Zhao, W. M., & Zhang, X. H. (2011). *Org. Electron.*, *12*, 2061.
[6] Kim, D., Zhu, L. Y., & Brédas, J. L. (2012). *Chem. Mater.*, *24*, 2604.
[7] Shang, X. H., Han, D. M., Li, D. F., & Wu, Z. J. (2013). *Chem. Phys. Lett.*, *565*, 12.
[8] Hwang, F. M., Chen, H. Y., Chen, P. S., Liu, C. S., Chi, Y., Shu, C. F., Wu, F. L., Chou, P. T., Peng, S. M., & Lee, G. H. (2005). *Inorg. Chem.*, *44*, 1344.
[9] Wu, W. T., Cheng, C. H., Wu, W. H., Guo, H. M., Ji, S. M., Song, P., Han, K. L., Zhao, J. Z., Zhang, X., Wu, Y. B., & Du, G. T. (2010). *Eur. J. Inorg. Chem.*, *29*, 4683.
[10] Su, J. J., Shi, L. L., Sun, X. B., Guan, W., & Wu, Z. J. (2011). *Dalton Trans.*, *40*, 11131.
[11] Wang, R. J., Deng, L. J., Zhang, T., & Li, J. Y. (2012). *Dalton Trans.*, *41*, 6833.
[12] Adachi, C., Baldo, M. A., Forrest, S. R., & Thompson, M. E. (2000). *Appl. Phys. Lett.*, *77*, 904.
[13] Adachi, C., Baldo, M. A., Forrest, S. R., Lamansky, S., Thompson, M. E., & Kwong, R. C. (2001). *Appl. Phys. Lett.*, *78*, 1622.
[14] Bergh, A., Craford, G., Duggal, A., & Haitz, R. (2001). *Phys. Today*, *54*, 42.
[15] Dedeian, K., Shi, J. M., Shepherd, N., Forsythe, E., & Morton, D. C. (2005). *Inorg. Chem.*, *44*, 4445.
[16] Tamayo, A. B., Alleyne, B. D., Djurovich, P. I., Lamansky, S., Tsyba, I., Ho, N. N., Bau, R., & Thompson, M. E. (2003). *J. Am. Chem. Soc.*, *125*, 7377.
[17] Avilov, I., Minoofar, P., Cornil, J., & De Cola, L. (2007). *J. Am. Chem. Soc.*, *129*, 8247.
[18] Su, S. J., Sasabe, H., Takeda, T., & Kido, J. (2008). *Chem. Mater.*, *20*, 1691.
[19] Orselli, E., Albuquerque, R. Q., Fransen, P. M., Froehlich, P., Janssen, H. M., & De Cola, L. (2008). *J. Mater. Chem.*, *18*, 4579.
[20] Hughes, G., & Bryce, M. R. (2005). *J. Mater. Chem.*, *15*, 94.
[21] Wang, C. S., Kilitziraki, M., Palsson, L. O., Bryce, M. R., Monkman, A. P., & Samuel, I. D. W. (2001). *Adv. Funct. Mater.*, *11*, 47.
[22] Chen, L. Q., You, H., Yang, C. L., Ma, D. G., & Qin, J. G. (2007). *Chem. Commun.*, 1352.
[23] Hohenberg, P., & Kohn, W. (1964). *Phys. Rev.*, *136*, B864.
[24] Becke, A. D. (1993). *J. Chem. Phys.*, *98*, 5648.
[25] Lee, C., Yang, W. T., & Parr, R. G. (1988). *Phys. Rev. B*, *37*, 785.
[26] Hay, P. J., & Wadt, W. R. (1985). *J. Chem. Phys.*, *82*, 270.
[27] Hay, P. J., & Wadt, W. R. (1985). *J. Chem. Phys.*, *82*, 299.
[28] O′Boyle, N. M., Tenderholt, A. L., & Langner, K. M. (2008). *J. Comput. Chem.*, *29*, 839.
[29] Avilov, I., Minoofar, P., Cornil, J., & De Cola, L. (2007). *J. Am. Chem. Soc.*, *129*, 8247.
[30] Shi, L. L., Geng, Y., Gao, H. Z., Su, Z. M., & Wu, Z. J. (2010). *Dalton Trans.*, *39*, 7733.
[31] Frisch, M. J. *et al.* (2009). *Gaussian 09*, Gaussian, Inc.: Wallingford, C T.
[32] Hush, N. S. (1958). *J. Chem. Phys.*, *28*, 962.
[33] Marcus, R. A. (1993). *Rev. Mod. Phys.*, *65*, 599.
[34] Marcus, R. A. (1956). *J. Chem. Phys.*, *24*, 966.
[35] Malagoli, M., & Brédas, J. L. (2000). *Chem. Phys. Lett.*, *327*, 13.
[36] Lin, B. C., Cheng, C. P., Ping, Z., & Lao, M. (2003). *J. Phys. Chem. A*, *107*, 5241.
[37] Sakanoue, K., Motoda, M., Sugimoto, M., & Sakaki, S. (1999). *J. Phys. Chem. A*, *103*, 5551.
[38] Lee, Y. Z., Chen, X. W., Chen, S. A., Wei, P. K., & Fann, W. S. (2001). *J. Am. Chem. Soc.*, *123*, 2296.
[39] Hutchison, G. R., Ratner, M. A., & Marks, T. J. (2005). *J. Am. Chem. Soc.*, *127*, 2339.
[40] Zhao, Y., & Truhlar, D. G. (2008). *Theor. Chem. Acc.*, *120*, 215.

Downloaded by [Xian Jiaotong University] at 13:23 11 December 2014